

JOINTLY OPTIMAL ARRAY GEOMETRIES AND WAVEFORMS IN ACTIVE SENSING: NEW INSIGHTS INTO ARRAY DESIGN VIA THE CRAMÉR-RAO BOUND

Ids van der Werf, Geert Leus

Robin Rajamäki

Delft University of Technology, The Netherlands

Aalto University, Finland

ABSTRACT

This paper investigates jointly optimal array geometry and waveform designs for active sensing. Specifically, we focus on minimizing the Cramér-Rao lower bound (CRB) of the angle of a single target in white Gaussian noise. We first find that several array-waveform pairs can yield the same CRB by virtue of sequences with equal sums of squares, i.e., solutions to certain Diophantine equations. Furthermore, we show that under physical aperture and sensor number constraints, the CRB-minimizing receive array geometry is unique, whereas the transmit array can be chosen flexibly. We leverage this freedom to design a novel sparse array geometry that not only minimizes the single-target CRB given an optimal waveform, but also has a nonredundant and contiguous sum co-array—a desirable property when launching independent waveforms, with relevance also to the multi-target case.

Index Terms— Active sensing, Cramér-Rao lower bound, sparse arrays, waveform design.

1. INTRODUCTION

Multisensor active sensing systems have recently experienced an increased research interest due to emerging applications such as automotive radar, and integrated sensing and communications [1, 2]. An important goal of such systems is high spatial resolution, including unambiguous and accurate direction-of-arrival (DoA) estimation, whereas key factors influencing performance are the *array geometry* and *transmit waveforms*. Among the numerous optimization criteria considered in literature, the Cramér-Rao lower bound (CRB) remains a popular choice as it provides a fundamental limit on unbiased DoA estimation performance. Past works have focused on (sparse array [3]) geometry optimization based on the CRB and related bounds in both passive [4–8] and active sensing [9–11], [3, Ch. 10], as well as transmit waveform optimization [12–16], [2, p. 220]. However, jointly optimal array geometries and transmit waveforms that minimize the CRB have not been investigated to the best of our knowledge. This paper seeks to address this gap by focusing on

the single-target CRB. The single-target case provides valuable insight with relevance also to the multi-target case, and applications such as beam alignment [17], target detection, and tracking [2, pp. 122, 422].

The contributions of the paper are as follows. Firstly, we show that *multiple* array-waveform pairs can yield *equal* CRBs, which follows from the realization that designing such array configurations corresponds to constructing integer sequences with equal sums of squares—a classical problem in number theory [18, 19]. Secondly, we derive the receive array geometry *minimizing* the CRB given a family of optimal waveforms corresponding to transmit beamforming, and certain physical constraints on the array aperture and number of sensors. We find a curious asymmetry between the transmitter and receiver: the optimal receive array is unique, whereas the transmit array can be chosen quite freely. We then leverage this freedom to design a novel jointly optimal sparse array geometry that also has a contiguous and nonredundant sum co-array. These properties are desirable for achieving high target identifiability and resolution in the general multi-target case when launching independent waveforms [20, 21].

2. BACKGROUND

2.1. Measurement model

We consider a monostatic active sensing multiple-input multiple output (MIMO) system consisting of N_t transmit (Tx) sensors collocated with N_r receive (Rx) sensors. Thus, the angle of incidence on the Rx array equals the angle of departure of the Tx array. Assuming a single target located in the far field of linear Tx and Rx arrays at unknown angle $\omega \in [-\pi, \pi)$, a narrowband received signal model is given by [20]

$$\mathbf{y} = (\mathbf{S} \otimes \mathbf{I})(\mathbf{a}_t(\omega) \otimes \mathbf{a}_r(\omega))\gamma + \mathbf{n}, \quad (1)$$

where \otimes denotes the Kronecker product, $\mathbf{S} \in \mathbb{C}^{T \times N_t}$ is a (known) spatio-temporal Tx waveform matrix, $T \geq 1$ is the waveform length in samples, $\gamma \in \mathbb{C}$ is the unknown reflection coefficient, and $\mathbf{n} \in \mathbb{C}^{N_r T}$ denotes an additive (spatio-temporally white) noise vector whose entries follow an i.i.d. circularly symmetric normal distribution with $\mathbb{E}(\mathbf{n}\mathbf{n}^H) = \sigma^2 \mathbf{I}$. Furthermore, $\mathbf{a}_t(\omega) = [e^{jd_t[1]\omega}, \dots, e^{jd_t[N_t]\omega}]^T$ and $\mathbf{a}_r(\omega) = [e^{jd_r[1]\omega}, \dots, e^{jd_r[N_r]\omega}]^T$ represent the steering vectors of the Tx and Rx arrays, respectively, whose sensor

This work was supported by the Netherlands Organisation for Applied Scientific Research, Netherlands Defence Academy (TNO-10026587), as well as projects Business Finland 6G-ISAC, Research Council of Finland FUN-ISAC (359094), and EU Horizon INSTINCT (101139161).

positions $\mathcal{D}_t = \{d_t[n]\}_{n=1}^{N_t} \subset \mathbb{Z}$ and $\mathcal{D}_r = \{d_r[m]\}_{m=1}^{N_r} \subset \mathbb{Z}$ are assumed to lie on a grid of integer multiples of half a carrier wavelength. Our goal is to estimate the target angle ω , and understand how the choice of Tx/Rx arrays $\mathcal{D}_t, \mathcal{D}_r$ and waveform matrix \mathbf{S} impact this task.

2.2. Single-target CRB and optimal transmit waveform

The single-target CRB of angle ω , assuming the reflection coefficient γ and noise power σ^2 are unknown nuisance parameters, can be shown to reduce to [22]

$$\text{CRB}(\omega) = \frac{\sigma^2}{2|\gamma|^2} \|\mathbf{P}_{\perp}^{\mathbf{S} \otimes \mathbf{I}} (\mathbf{S} \otimes \mathbf{I}) \dot{\mathbf{a}}_{\text{tr}}(\omega)\|_2^{-2}. \quad (2)$$

Here, $\mathbf{P}_{\perp}^{\mathbf{X}}$ denotes the projection onto the orthogonal complement of the range space of \mathbf{X} ; $\mathbf{a}_{\text{tr}}(\omega) \triangleq \mathbf{a}_t(\omega) \otimes \mathbf{a}_r(\omega)$ is the effective Tx-Rx steering vector; and $\dot{\mathbf{a}}_{\text{tr}}(\omega) \triangleq \frac{\partial}{\partial \omega} \mathbf{a}_{\text{tr}}(\omega)$ is its derivative with respect to ω . Forsythe and Bliss [12], as well as Li *et al.* [13], investigated waveforms \mathbf{S} minimizing the CRB given an array geometry. In the single-target case (2), the optimal waveform depends on the “spatial variances” of the Tx and Rx arrays [12], $\chi_t \triangleq \chi(\mathcal{D}_t)$ and $\chi_r \triangleq \chi(\mathcal{D}_r)$, where

$$\chi(\mathcal{D}) \triangleq \frac{1}{|\mathcal{D}|} \sum_{d \in \mathcal{D}} (d - \mu(\mathcal{D}))^2, \quad (3)$$

and the corresponding spatial mean is $\mu(\mathcal{D}) \triangleq \frac{1}{|\mathcal{D}|} \sum_{d \in \mathcal{D}} d$. In particular, if the following condition is satisfied:

$$\chi_r > \chi_t, \quad (4)$$

then the optimal waveform matrix has the form [12]:

$$\mathbf{S}_o \triangleq \arg \min_{\mathbf{S} \in \mathbb{C}^{T \times N_t}} \{\text{CRB}(\omega) : \chi_r > \chi_t, \|\mathbf{S}\|_{\text{F}}^2 \leq 1\} = \frac{\mathbf{u} \mathbf{a}_{\text{tr}}^{\text{H}}(\omega)}{\sqrt{N_t}}, \quad (5)$$

where $\mathbf{u} \in \mathbb{C}^T$ is an arbitrary unit norm vector ($\|\mathbf{u}\|_2 = 1$), and the Tx power $\|\mathbf{S}\|_{\text{F}}^2$ is w.l.o.g. constrained to ≤ 1 . Eq. (5) simply corresponds to fully coherent transmission in the target direction ω , i.e., *Tx beamforming*. If $\chi_r = \chi_t$, then optimal waveforms beyond (5) also exist [13]. Otherwise, if $\chi_r < \chi_t$, then the optimal waveform corresponds to transmitting infinitesimal energy in the target direction—see [12, 13] for details. As this solution has limited practical relevance, we will henceforth focus on (5) which is optimal given (4).

We conclude by highlighting two interesting facts revealed by (5). Firstly, any optimal waveform matrix is column rank-deficient (when $N_t > 1$). Hence, widely employed *orthogonal waveforms do not generally minimize the CRB*—even in the case of multiple targets [13]. Secondly, any optimal waveform depends on the Tx array geometry \mathcal{D}_t (and true target angle ω) via steering vector $\mathbf{a}_t(\omega)$. That is, *different Tx arrays lead to different optimal waveforms*. While this was observed in [12, 13], the impact of the array geometry on the CRB was not fully explored. Hence, we attempt to fill this gap by asking *which Tx/Rx array geometries minimize the CRB in (2) jointly with the optimal waveform in (5)?*

3. JOINTLY OPTIMAL ARRAY-WAVEFORM PAIRS

3.1. Equal CRB via Rx arrays with equal sums of squares

Substituting the optimal waveform in (5) into (2) can be shown to simplify the single-target CRB into [12]

$$\text{CRB}(\omega) = \frac{\sigma^2}{2|\gamma|^2} \frac{1}{N_t N_r} \chi_r^{-1}. \quad (6)$$

Hence, the CRB (given an optimal waveform) is independent of the target angle ω and only depends on the Tx array geometry via the number of Tx sensors, N_t . In contrast, for a fixed number of Rx sensor N_r , the CRB depends on the Rx array geometry via its spatial variance, χ_r . This suggests an intriguing possibility: Rx array geometries with equal spatial variances yield equal CRBs. Designing such arrays actually corresponds to finding integer sequences with *equal sums of squares*—a special class of Diophantine equations that have a long history in number theory [18, 19]. For example, $1^2 + 8^2 = 4^2 + 7^2$ can be used to construct arrays $\mathcal{D}_1 = \{-8, -1, 1, 8\}$ and $\mathcal{D}_2 = \{-7, -4, 4, 7\}$ satisfying $\chi(\mathcal{D}_1) = \chi(\mathcal{D}_2)$. While *different* array geometries can achieve the *same* CRB, their practical DoA estimation performance may differ, as Section 4 will demonstrate. Fully exploring this prospect is left for future work. Instead, we now turn our attention to deriving the Rx array configuration minimizing the CRB (6).

3.2. Optimal Rx array geometry: Clustered array

The CRB in (6) is a monotonically decreasing function in increasing χ_r . Since the CRB can be made arbitrarily small simply by expanding the Rx aperture without bound, a more meaningful question is: which array geometry is optimal under a constraint on the physical array aperture? To answer this question, we make use of the following Lemma, which shows that the sparse array geometry whose sensors are clustered around the extremes of the array maximizes the spatial variance under an aperture constraint. For simplicity and brevity, we denote the set of nonnegative integers smaller than N , i.e., the N -sensor uniform linear array (ULA), by $\mathcal{U}_N \triangleq \{0, 1, \dots, N-1\}$, and focus on the case of *even* N .

Lemma 1 (Clustered array). *Let $\mathcal{L} = \mathcal{U}_{L+1}$, where $L \in \mathbb{N}_+$ is fixed. Then, given an even $N \leq L+1$, the subset $\mathcal{D} \subseteq \mathcal{L}$ of size $|\mathcal{D}| = N$ maximizing $\chi(\mathcal{D})$ in (3) is $\mathcal{D} = \mathcal{K}_N^L$, where*

$$\mathcal{K}_N^L \triangleq \arg \min_{\mathcal{D} \subseteq \mathcal{L}} \{\chi(\mathcal{D}) : |\mathcal{D}| = N\} = \mathcal{U}_{N/2} \cup (L - \mathcal{U}_{N/2}). \quad (7)$$

Moreover, the (optimal) value of the spatial variance is

$$\chi(\mathcal{K}_N^L) = \frac{1}{4} \left((L+1 - \frac{N}{2})^2 + \frac{1}{3} (\frac{N^2}{4} - 1) \right). \quad (8)$$

The proof of (7) follows directly via negation and is omitted for brevity. Similarly, the value of $\chi(\mathcal{K}_N^L)$ follows by straightforward computation after substituting (7) into (3).

We can now characterize the set of array-waveform pairs jointly minimizing the single-target CRB (2), i.e., solutions to

$$\underset{\substack{\mathcal{D}_t, \mathcal{D}_r \subset \mathbb{C}^N \\ \mathbf{S} \in \mathbb{C}^{T \times N_t}}}{\text{minimize}} \text{CRB}(\omega) \text{ s.t. } \begin{cases} |\mathcal{D}_t| = N_t, |\mathcal{D}_r| = N_r, \\ \|\mathbf{S}\|_{\text{F}}^2 \leq 1, \\ \max \mathcal{D}_r - \min \mathcal{D}_r \leq L, \\ \chi(\mathcal{D}_r) > \chi(\mathcal{D}_t). \end{cases} \quad (9)$$

In addition to the number of Tx/Rx sensors and Tx power, we have also constrained the Rx aperture (to $\leq L$). Moreover, the spatial variance of the Tx array should be smaller than that of the Rx array to ensure that Tx beamforming (5) is optimal.

Theorem 1 (Jointly optimal array-waveform pairs). *Suppose (9) is feasible for given $N_t, N_r, L \in \mathbb{N}_+$, where N_r is even. Then the solutions $(\mathcal{D}_t^*, \mathcal{D}_r^*, \mathbf{S}^*)$ to (9) are: \mathbf{S}^* given by (5),*

$$\mathcal{D}_r^* = \mathcal{K}_{N_r}^L \quad (10)$$

given by (7), and any \mathcal{D}_t^* satisfying (4) and $|\mathcal{D}_t^*| = N_t$.

Proof. Per [12], (5) is optimal when (4) holds. Hence, the CRB (2) simplifies to (6). By Lemma 1, (6) is minimized by (10), when the Rx aperture is $\leq L$. Finally, any \mathcal{D}_t satisfying (4) and $|\mathcal{D}_t| = N_t$ has the same CRB, and is thus optimal. \square

Remark 1. *By Theorem 1, the clustered array in (10) is the unique optimal Rx array, whereas several optimal waveforms and Tx arrays exist: \mathbf{S}^* follows (5) and therefore depends on \mathcal{D}_t^* , which can be chosen freely provided it satisfies (4).*

The subtle question remains for which values of tuple (N_t, N_r, L) optimization problem (9) is feasible? A simple sufficient condition is $N_t \leq N_r \leq L + 1$, since then the feasible set of (9) contains $\mathcal{D}_r = \mathcal{U}_{N_r}$ and $\mathcal{D}_t = \mathcal{U}_{N_t}$, which trivially satisfy (4). Deriving necessary and sufficient conditions in terms of (N_t, N_r, L) is beyond the scope of this paper and left for future work. Instead, we now turn our attention to how to pick an optimal Tx array among the possible choices.

3.3. How should the Tx array geometry be chosen?

The minimum single-target CRB—jointly optimized over the waveform and array geometry—may be achieved by multiple choices of the Tx array (cf. Remark 1). Nevertheless, some Tx array configurations might be preferable over others in terms of performance indicators beyond the CRB. Herein, we consider *identifiability*, which quantifies if for a fixed number of K targets, any given (noiseless) measurement can be associated with a unique set of DoAs. In active sensing, identifiability depends on the geometry of the sum co-array [21]:

$$\mathcal{D}_\Sigma \triangleq \mathcal{D}_t + \mathcal{D}_r = \{d_t + d_r \mid d_t \in \mathcal{D}_t; d_r \in \mathcal{D}_r\}.$$

Let $N_\Sigma \triangleq |\mathcal{D}_\Sigma|$ denote the number of sum co-array elements. A sufficient condition for identifying any $K \leq N_\Sigma/2$ targets

is that the sum co-array is *contiguous* and the Tx waveform has full column rank, i.e., $\mathcal{D}_\Sigma = \mathcal{U}_{N_\Sigma}$ and $\text{rank}(\mathbf{S}) = N_t$ [23]. Since $N_\Sigma \leq N_t N_r$, up to $N_t N_r/2$ targets can be identified by a contiguous sum co-array with appropriately chosen (e.g., orthogonal) waveforms.¹ An array achieving $N_\Sigma = N_t N_r$ is called *nonredundant*. The following Corollary establishes a set of (N_t, N_r, L) tuples solving (9) and yielding a contiguous and nonredundant sum co-array. For a proof, see Appendix A.

Corollary 1 (Optimal contiguous nonredundant co-array). *Given $N_t, N_r \in \mathbb{N}_+$, where N_r is even, if $L = (N_t + 1)N_r/2 - 1$, then the following Tx array is a solution to (9):*

$$\mathcal{D}_t^* = \frac{N_r}{2} \mathcal{U}_{N_t}. \quad (11)$$

The sum co-array of (11) and the optimal Rx array (10) is contiguous ($\mathcal{D}_\Sigma = \mathcal{U}_{N_\Sigma}$) and nonredundant ($N_\Sigma = N_t N_r$).

To the best of our knowledge, the sparse Tx-Rx array geometry in (10) and (11) has not appeared in the literature before. Neither has its optimality w.r.t. minimizing the single-target CRB been established, nor the fact that it can achieve a contiguous nonredundant sum co-array. We note that the clustered array in (7) has empirically [5] been found to minimize the so-called *unconditional* CRB corresponding to a different (single-target) measurement model typically arising in passive sensing. This is nevertheless different from the active sensing model (1) and *conditional* CRB considered herein, and hence does not imply our results. Moreover, in stark contrast to passive sensing, in active sensing one has the freedom to choose both the Tx array geometry (as in Section 3.3) and the transmitted waveforms, despite the optimal Rx array being a clustered array in both cases. Exploring generalizations of the array geometry in (10) and (11) is left for future work. Such generalizations, possibly with a redundant or even noncontiguous sum co-array, may be of interest in minimizing the CRB given an \mathbf{S} differing from the (optimal) choice in (5).

4. NUMERICAL EXAMPLES

Next, we illustrate the results of Section 3 numerically. We focus on the four array geometries depicted in Fig. 1, where (a) shows the optimal array defined by (10) and (11). We consider the maximum-likelihood estimator (MLE) of ω for a *fixed* waveform matrix \mathbf{S} . Given (1), the MLE can be shown to reduce to the following joint Tx-Rx beamformer [24]: $\hat{\omega} = \arg \max_{\omega \in [-\pi, \pi]} |\mathbf{y}^H(\mathbf{S}\mathbf{a}_t(\bar{\omega}) \otimes \mathbf{a}_r(\bar{\omega}))|^2 / \|\mathbf{S}\mathbf{a}_t(\bar{\omega})\|_2^2$. We assume the optimal waveform in (5) is used, with $\mathbf{u} = \frac{1}{\sqrt{T}} \mathbf{1}_T$ and $T = N_t$. Since \mathbf{S} is a function of the true angle, an initial estimate of ω would be needed in practice; see [13] for a discussion and examples. The ground truth target angle and reflectivity are set to $\omega = 0$ and $\gamma = 1$, respectively, whereas entries of noise vector \mathbf{n} are drawn from an i.i.d. circularly symmetric normal distribution with variance σ^2 . The squared error of the MLE is averaged over 10^4 Monte Carlo trials.

¹ Fully leveraging the sum co-array would hence in general require transmitting a suboptimal waveform, i.e., one that does not minimize the CRB.

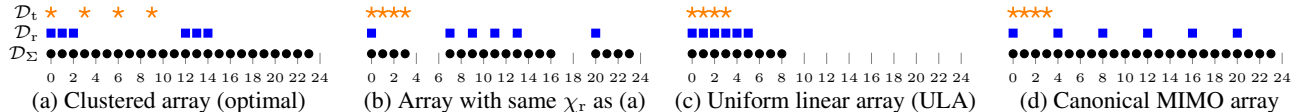


Fig. 1: Array geometries with $N_t = 4$ transmitter and $N_r = 6$ receiver sensors. Array (a) maximizes the Rx spatial variance χ_r given physical aperture $L = 14$, and has a contiguous nonredundant sum co-array. The Rx array in (b) has equal χ_r , but larger L .

Fig. 2 shows the (single-target) CRBs and empirical MLE performance of the array configurations in Fig. 1 as a function of SNR $\triangleq 10 \log(|\gamma|^2/\sigma^2)$. The optimal array in Fig. 1(a) minimizes the CRB among all geometries with aperture $L = 14$. By using a larger aperture, one can construct array configurations achieving *equal* or larger CRB, as the array in Fig. 1(b) with $L = 20$ shows. Indeed, the spatial variances of the Rx arrays in (a) and (b) are identical by virtue of the following equal sums of squares: $5^2 + 6^2 + 7^2 = 1^2 + 3^2 + 10^2$. Although the CRBs of arrays (a) and (b) are identical, their MLE performance in the threshold region differs. This is related to the difference in the beampatterns of the two arrays. Understanding exactly how the array geometry affects MLE, especially for arrays with equal spatial variance in (3), is an open question. Finally, we contrast the clustered array in Fig. 1 (a) to the well-known (c) ULA and (d) canonical MIMO (radar) array with a nested structure. The ULA has a significantly higher CRB than the other arrays due to its smaller spatial variance. In contrast, the MIMO array, due to its larger Rx aperture ($L = 20$), has a slightly lower CRB than the clustered array in (a). However, the clustered array requires *only half the physical aperture* to realize the same sum co-array. This is advantageous when high identifiability and angular resolution yet small physical array size is desirable, as in automotive radar [1]. The MLE of the MIMO array suffers from poor performance due to spatial aliasing, as its Rx array (a dilated ULA) lacks consecutive elements, unlike the Clustered array. Although the issue can be alleviated by restricting the search space of the MLE to the vicinity of ω based on the region illuminated upon Tx, it also illustrates that upon coherent transmission, angle estimation performance heavily depends on the Rx array geometry, as opposed to the sum co-array which is key when transmitting independent waveforms [21]. Judicious array design is thus needed to ensure robust performance across various transmission strategies.

5. CONCLUSION

This paper investigated waveform-array geometry pairs minimizing the single-target CRB in active sensing. Focusing on a family of optimal waveforms [12, 13] corresponding to Tx beamforming in the target direction, we showed that the optimal linear Rx array places sensors at the edges of its aperture to maximize its spatial variance—the sums of squares of its centered sensor positions. The Tx array geometry can be chosen freely, provided its spatial variance does not exceed that of the Rx array. We established that the Tx array can be selected such that the sum co-array of the joint Tx-Rx array is

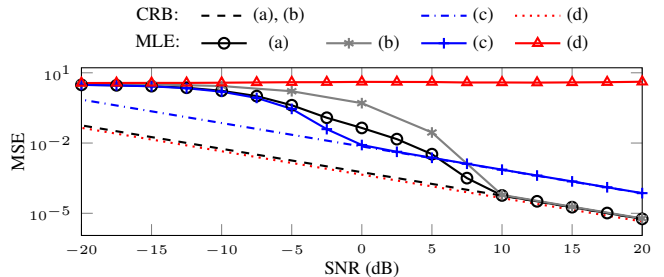


Fig. 2: Single-target CRB and MLE performance of array geometries in Fig. 1 using an optimal waveform following (5).

both contiguous and nonredundant. The derived array geometry therefore has optimal properties both (in the single and multi-target cases) when launching coherent and independent waveforms, in contrast to the ULA, which has substantially higher CRB and lower identifiability, and the (nonredundant nested) MIMO array, which requires a larger physical aperture to achieve a comparable CRB and sum co-array.

A. PROOF OF COROLLARY 1

We first show that if $L = (N_t + 1)N_r/2 - 1$ then (11) is a solution of (9). This reduces to showing that (11) satisfies (4) given $\mathcal{D}_r^* = \mathcal{K}_{N_r}^L$, which Theorem 1 established was the optimal Rx array configuration. By (3), we have

$$\chi(\mathcal{D}_r^*) = \chi\left(\frac{N_r}{2}\mathcal{U}_{N_r}\right) = \frac{N_r^2}{4}\chi(\mathcal{U}_{N_r}) = \frac{1}{48}(N_t^2 - 1)N_r^2. \quad (12)$$

Since $\mathcal{D}_r^* = \mathcal{K}_{N_r}^L$, where $L = (N_t + 1)N_r/2 - 1$, condition $\chi(\mathcal{D}_r^*) > \chi(\mathcal{D}_r^*)$ can be rewritten using (8) and (12) as

$$\frac{1}{4}\left(\left(\frac{N_t N_r}{2}\right)^2 + \frac{1}{3}\left(\frac{N_t^2}{4} - 1\right)\right) > \frac{1}{48}(N_t^2 - 1)N_r^2.$$

Rearranging terms yields $2N_r^2(N_t^2 + 1) - 4 > 0$, which holds for any even $N_r \geq 2$. Hence, (4) is satisfied, which implies that the feasible set of (9) is nonempty, and per Theorem 1, that (11) is an optimal solution to (9).

We now show that the sum co-array is contiguous and nonredundant. Let $\alpha = N_r/2$ and $\beta = N_t\alpha = N_t N_r/2$. Then

$$\begin{aligned} \mathcal{D}_\Sigma &= \alpha\mathcal{U}_{N_t} + (\mathcal{U}_\alpha \cup (L - \mathcal{U}_\alpha)) \\ &= (\alpha\mathcal{U}_{N_t} + \mathcal{U}_\alpha) \cup (\alpha\mathcal{U}_{N_t} - \mathcal{U}_\alpha + L), \end{aligned}$$

where $\alpha\mathcal{U}_{N_t} + \mathcal{U}_\alpha = \{\alpha m + n \mid m \in \mathcal{U}_{N_t}; n \in \mathcal{U}_\alpha\} = \mathcal{U}_\beta$. Furthermore, note that $-\mathcal{U}_M = \mathcal{U}_M - M + 1$. Hence,

$$\alpha\mathcal{U}_{N_t} - \mathcal{U}_\alpha + L = \alpha\mathcal{U}_{N_t} + \mathcal{U}_\alpha + L - \alpha + 1.$$

Recalling that $L = \beta + \alpha - 1$ then yields the desired result

$$\mathcal{D}_\Sigma = \mathcal{U}_\beta \cup (\mathcal{U}_\beta + \beta) = \mathcal{U}_{2\beta} = \mathcal{U}_{N_t N_r}. \quad \square$$

6. REFERENCES

- [1] S. Sun, A. P. Petropulu, and H. V. Poor, “MIMO radar for advanced driver-assistance systems and autonomous driving: Advantages and challenges,” *IEEE Signal Process. Mag.*, vol. 37, no. 4, pp. 98–117, 2020.
- [2] F. Liu, C. Masouros, and Y. C. Eldar, *Integrated Sensing and Communications*, Springer Singapore, 2023.
- [3] M. G. Amin, Ed., *Sparse Arrays for Radar, Sonar, and Communications*, Wiley-IEEE, 2024.
- [4] C. Chambers, T. C. Tozer, K. C. Sharman, and T. S. Durani, “Temporal and spatial sampling influence on the estimates of superimposed narrowband signals: when less can mean more,” *IEEE Trans. Signal Process.*, vol. 44, no. 12, pp. 3085–3098, 1996.
- [5] A. B. Gershman and J. F. Böhme, “A note on most favorable array geometries for DOA estimation and array interpolation,” *IEEE Signal Process. Lett.*, vol. 4, no. 8, pp. 232–235, 1997.
- [6] V. Roy, S. P. Chepuri, and G. Leus, “Sparsity-enforcing sensor selection for DOA estimation,” in *Proc. of the IEEE Int. Workshop Computat. Advances Multi-Sensor Adaptive Process. (CAMSAP)*, 2013, pp. 340–343.
- [7] R. R. Pote and B. D. Rao, “Reduced dimension beamspace design incorporating nested array for mmwave channel estimation,” in *Asilomar Conf. Signals, Syst. and Comput.*, 2019, pp. 1212–1216.
- [8] C. A. Kokke, M. Coutino, L. Anitori, R. Heusdens, and G. Leus, “Sensor selection for angle of arrival estimation based on the two-target Cramér-Rao bound,” in *Proc. of the IEEE Int. Conf. on Acoustics, Speech and Signal Process. (ICASSP)*, 2023, pp. 1–5.
- [9] Qian He, Rick S. Blum, Hana Godrich, and Alexander M. Haimovich, “Target velocity estimation and antenna placement for MIMO radar with widely separated antennas,” *IEEE J. Sel. Topics Signal Process.*, vol. 4, no. 1, pp. 79–100, 2010.
- [10] E. Tohidi, M. Coutino, S. P. Chepuri, H. Behroozi, M. M. Nayebi, and G. Leus, “Sparse antenna and pulse placement for colocated MIMO radar,” *IEEE Trans. Signal Process.*, vol. 67, no. 3, pp. 579–593, 2019.
- [11] J. Tabrikian, O. Isaacs, and I. Bilik, “Cognitive antenna selection for automotive radar using Bobrovsky-Zakai bound,” *IEEE J. Sel. Topics Signal Process.*, vol. 15, no. 4, pp. 892–903, 2021.
- [12] K.W. Forsythe and D.W. Bliss, “Waveform correlation and optimization issues for MIMO radar,” in *Asilomar Conf. Signals, Syst. and Comput.*, 2005, pp. 1306–1310.
- [13] J. Li, L. Xu, P. Stoica, K. W. Forsythe, and D. W. Bliss, “Range compression and waveform optimization for MIMO radar: A Cramér-Rao bound based study,” *IEEE Trans. Signal Process.*, vol. 56, no. 1, pp. 218–232, 2008.
- [14] M. Bică and V. Koivunen, “Radar waveform optimization for target parameter estimation in cooperative radar-communications systems,” *IEEE Trans. Aero. and Electr. Syst.*, vol. 55, no. 5, pp. 2314–2326, 2019.
- [15] X. Li, V. C. Andrei, U. J. Mönich, and H. Boche, “Optimal and robust waveform design for MIMO-OFDM channel sensing: A Cramér-Rao bound perspective,” in *IEEE Int. Conf. Commun. (ICC)*, 2023, pp. 3516–3521.
- [16] I. van der Werf, R. C. Hendriks, R. Heusdens, and G. Leus, “Transmit waveform design based on the Cramér-Rao lower bound,” in *Proc. of the IEEE Int. Workshop Computat. Advances Multi-Sensor Adaptive Process. (CAMSAP)*, 2023, pp. 166–170.
- [17] S.-E. Chiu, N. Ronquillo, and T. Javidi, “Active learning and CSI acquisition for mmWave initial alignment,” *IEEE J. Sel. Areas Commun.*, vol. 37, no. 11, pp. 2474–2489, 2019.
- [18] I. A. Barnett and C. W. Mendel, “On equal sums of squares,” *The American Mathematical Monthly*, vol. 49, no. 3, pp. 157–170, 1942.
- [19] C. J. Bradley, “82.7 equal sums of squares,” *The Mathematical Gazette*, vol. 82, no. 493, pp. 80–85, 1998.
- [20] I. Bekkerman and J. Tabrikian, “Target detection and localization using MIMO radars and sonars,” *IEEE Trans. Signal Process.*, vol. 54, no. 10, pp. 3873–3883, 2006.
- [21] J. Li, P. Stoica, L. Xu, and W. Roberts, “On parameter identifiability of MIMO radar,” *IEEE Signal Process. Lett.*, vol. 14, no. 12, pp. 968–971, 2007.
- [22] P. Stoica and A. Nehorai, “MUSIC, maximum likelihood, and Cramer-Rao bound,” *IEEE Trans. Acoust., Speech, Signal Process.*, vol. 37, no. 5, pp. 720–741, 1989.
- [23] R. Rajamäki and P. Pal, “Importance of array redundancy pattern in active sensing,” in *Proc. of the IEEE Int. Workshop Computat. Advances Multi-Sensor Adaptive Process. (CAMSAP)*, 2023.
- [24] J. E. Evans, D. F. Sun, and J. R. Johnson, “Application of advanced signal processing techniques to angle of arrival estimation in ATC navigation and surveillance systems,” Tech. Rep. 582, Massachusetts Inst of Tech Lexington Lincoln Lab, 1982.